

PERMUTATION DETECTORS UNDER CORRELATED K-DISTRIBUTED CLUTTER IN RADAR APPLICATIONS

José E. González-García*, José L. Sanz-González** and Francisco Álvarez-Vaquero**

Universidad Politécnica de Madrid (UPM)

* DIAC - EUIT de Telecomunicación-UPM. Ctra. Valencia km 7, 28031 – Madrid. SPAIN

Phone, Fax: +34 91 336 77 99, 77 84 Email: jegonzal@diac.upm.es

web: www.diac.upm.es

** Dpto. SSR - ETSI de Telecomunicación-UPM. Ciudad Universitaria, 28040 – Madrid. SPAIN

ABSTRACT

In this paper, we analyze the performance of some permutation tests (PTs) under a correlated K-distributed clutter model and nonfluctuating and Swerling II target models. Also, we compare the PTs results against their parametric counterparts under the same conditions. We analyze the detector performances in terms of detection probability (P_d) versus signal-to-clutter ratio (SCR) for different parameter values: the number of integrated pulses (N), the clutter reference samples (M), the false alarm probability (P_{fa}), the shape parameter (ν) of the K-distributed clutter and the clutter correlation coefficients.

1. INTRODUCTION

A permutation test is a nonparametric test, which is distribution-free under independent and identically distributed (IID) samples, because the distribution of a block of IID samples is invariant under the permutation of its sample components; then, permutation detectors (tests) are nonparametric CFAR (Constant False-Alarm Rate) detectors if clutter samples are IID. Also, the optimum statistic for the parametric detector is also optimum for the permutation detector, as it was proved in [1].

Suppose that the signal comes from a two-dimensional pulsed-radar system and we shall consider a non-coherent detection approach (i.e. the envelope of the received signal). In order to test hypothesis H_0 (target absent) against hypothesis H_1 (target present) for each azimuth in a specific range cell, we take M reference samples corresponding to the range cells surrounding the cell under test. Also, we consider a block of N pulses for each azimuth (corresponding to the number of pulses per antenna beamwidth), then, for each pulse i we have the vector of samples

$$\mathbf{x}_i = (x_{i1}, x_{i2}, \dots, x_{iM}, x_i), \quad i = 1, 2, \dots, N \quad (1)$$

where the last component x_i of vector \mathbf{x}_i is the sample of the range cell under test. (The range cell under test is in the middle of the reference range cells).

The performance analysis of the permutation tests (PTs) under K-distributed clutter and IID samples was already presented in [1]. Here, we analyze only the performance of some

PTs under a correlated K-distributed clutter model and nonfluctuating (NF) and Swerling II (SW-II) target models.

2. ANALYSIS UNDER CORRELATED K-DISTRIBUTED CLUTTER

We analyze the performances of our permutation detectors under correlated clutter. The sample correlation is introduced in the “in phase” and “quadrature” components by means of linear filtering of Gaussian processes [2]. Note that we generate K-distributed clutter from a complex Gaussian process multiplied by a process with chi-distribution, which is also obtained from 2ν independent Gaussian processes, being ν ($\nu = 0.5, 1, 1.5, 2, \dots, \infty$) the shape parameter of the distribution. If \tilde{W} is a complex Gaussian random variable and Y is a real chi-distributed random variable independent of \tilde{W} , then $\tilde{X} = \tilde{W} \cdot Y$ is a complex K-distributed random variable. More over, it is well known that random variable Y can be expressed by $Y = \sqrt{(Z_1^2 + Z_2^2 + \dots + Z_{2\nu}^2)/2\nu}$, where Z_k , $k = 1, 2, \dots, 2\nu$, are independent Gaussian random variables, being ν the shape parameter of the chi-distribution.

In order to introduce the correlation among samples, we consider sequences, i.e.

$$\begin{aligned} \tilde{X}(n) &= \tilde{W}(n) \cdot Y(n), \\ Y(n) &= \sqrt{\frac{1}{2\nu} [Z_1^2(n) + Z_2^2(n) + \dots + Z_{2\nu}^2(n)]} \end{aligned} \quad (2)$$

Considering first-order filters for processing $\tilde{W}(n)$ and $Z_k(n)$, $k = 1, 2, \dots, 2\nu$, we have

$$\begin{aligned} \tilde{W}(n) &= \rho_1 \cdot \tilde{W}(n-1) + \sqrt{1 - \rho_1^2} \cdot \tilde{W}_0(n), \quad 0 \leq \rho_1 \leq 1 \\ Z_k(n) &= \rho_2 \cdot Z_k(n-1) + \sqrt{1 - \rho_2^2} \cdot Z_{0k}(n), \quad 0 \leq \rho_2 \leq 1 \end{aligned} \quad (3)$$

where $\tilde{W}_0(n)$ is a complex white Gaussian process of unit power in each component, and $Z_{0k}(n)$, $k = 1, 2, \dots, 2\nu$ are independent real white Gaussian processes of unit power. Note that ρ_1 and ρ_2 are the one-lag correlation coefficients, and $\tilde{W}(n)$ and $Z_k(n)$, $k = 1, 2, \dots, 2\nu$ have exponential auto-correlation function and unit power.

For a block of N pulses with $M+1$ samples per pulse, we have to apply (3) in range and in azimuth (two-dimensional filtering), i.e.

$$\tilde{W}'(i, j) = \rho_{11} \cdot \tilde{W}'(i, j-1) + \sqrt{1-\rho_{11}^2} \cdot \tilde{W}_0(i, j), 0 \leq \rho_{11} \leq 1 \quad (4)$$

$$\tilde{W}(i, j) = \rho_{21} \cdot \tilde{W}(i-1, j) + \sqrt{1-\rho_{21}^2} \cdot \tilde{W}'(i, j), 0 \leq \rho_{21} \leq 1$$

where $\tilde{W}_0(i, j)$ is a complex two-dimensional white Gaussian process, ρ_{11} and ρ_{21} are the correlation coefficients in range j and in azimuth i , respectively, for the factor \tilde{W} . On the other hand,

$$Z'_k(i, j) = \rho_{12} \cdot Z'_k(i, j-1) + \sqrt{1-\rho_{12}^2} \cdot Z_{0k}(i, j), 0 \leq \rho_{12} \leq 1 \quad (5)$$

$$Z_k(i, j) = \rho_{22} \cdot Z_k(i-1, j) + \sqrt{1-\rho_{22}^2} \cdot Z'_k(i, j), 0 \leq \rho_{22} \leq 1$$

where $Z_{0k}(i, j)$, $k=1, 2, \dots, 2\nu$ are independent two-dimensional white Gaussian processes, ρ_{12} and ρ_{22} are the correlation coefficients in range j and in azimuth i , respectively, for each $Z_k(i, j)$, $k=1, 2, \dots, 2\nu$.

Finally, the clutter envelope samples x_{ij} , $i=1, 2, \dots, N$; $j=1, 2, \dots, M+1$ are obtained from

$$Y(i, j) = \sqrt{\frac{1}{2\nu} [Z_1^2(i, j) + Z_2^2(i, j) + \dots + Z_{2\nu}^2(i, j)]}$$

$$x_{ij} = |\tilde{W}(i, j)| \cdot Y(i, j) \quad (6)$$

$$i=1, 2, \dots, N; \quad j=1, 2, \dots, M+1$$

Note that $x_i = x_{ij}$ for $j = \lfloor (M+1)/2 \rfloor$

In our simulations, we have considered the four correlation coefficients and, in order to simplify the nomenclature, we define $Ro = [\rho_{11}, \rho_{12}, \rho_{21}, \rho_{22}]$. Then $Ro = [0, 0, 0, 0]$ corresponds to IID conditions, $Ro = [\rho_{11}, \rho_{12}, 0, 0]$ corresponds to correlation only in range, $Ro = [0, 0, \rho_{21}, \rho_{22}]$ corresponds to correlation only in azimuth and $Ro = [\rho_{11}, 1, \rho_{21}, 1]$ corresponds to Spherically Invariant Random Process (SIRP) clutter model [3-6].

3. SIMULATION RESULTS

In this paper, we present results of P_d versus signal-to-clutter ratio (SCR) for parametric tests against permutation tests with linear, quadratic, logarithmic and clipping statistics under K-distributed clutter [1-4], and nonfluctuating and Swerling II target models, considering $P_{fa}=10^{-3}$ and one value for the parameters N and M : $N=8$ and $M=7$.

According to [1], consider the following test statistic

$$T(\mathbf{x}) = \sum_{i=1}^N a_i(x_i), \text{ and define the linear statistic: } a_i(x) = x,$$

the quadratic statistic: $a_i(x) = x^2$, the logarithmic statistic: $a_i(x) = \log(1 + \alpha \cdot x)$ where α is a parameter, and the clipping statistic [7]:

$$a_i(x) = x - |x - A| = \begin{cases} (2x - A), & \text{if } 0 \leq x < A \\ A, & \text{if } x \geq A \end{cases}$$

where A is a clipping parameter. The detector is the implementation of the test:

$$T(\mathbf{x}) \begin{matrix} > \\ < \end{matrix} T_0 \begin{matrix} H_1 \\ H_0 \end{matrix}$$

Let us define the detectability loss (L , in dB) of a detector with respect to the parametric optimum one, as follows:

$$L(P_d, P_{fa}, N, M, \nu) = SCR(P_d, P_{fa}, N, M, \nu) - SCR_{opt}(P_d, P_{fa}, N, \nu) \quad (7)$$

where SCR and SCR_{opt} are signal-to-clutter ratios of the considered detector and the parametric optimum detector, respectively, depending on the parameters shown.

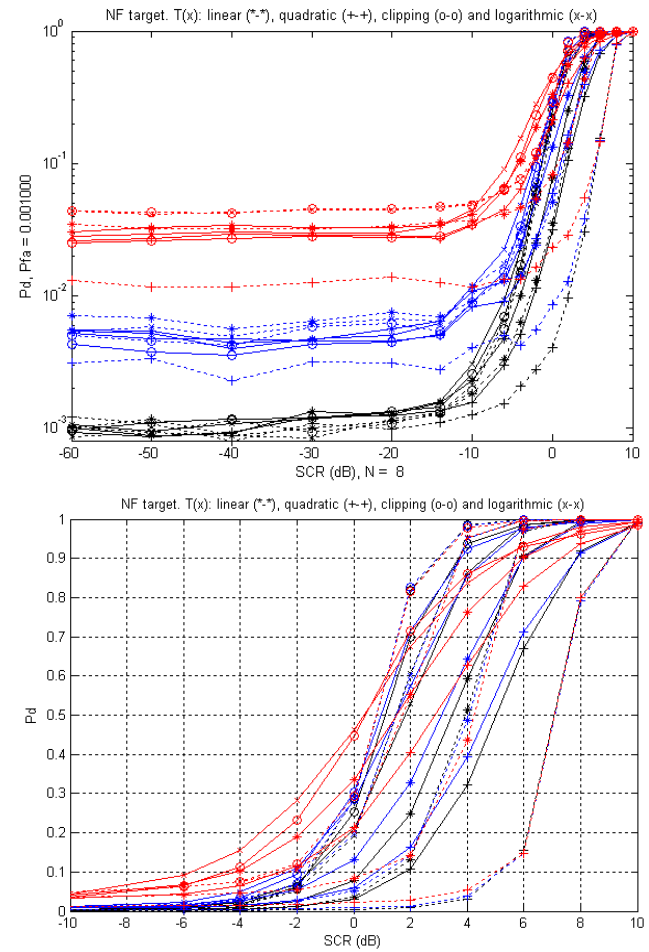


Figure 1 - Detection probability (P_d) versus SCR for parametric (dotted lines) and permutation (continuous lines) detectors ($N=8$ and $M=7$), under correlated spiky clutter ($\nu=0.5$) and nonfluctuating target model (NF). Picture on the top has log-scale for P_d while picture on the bottom has linear-scale for P_d . Clutter correlation coefficients: $Ro = [\rho_{11}, \rho_{12}, \rho_{21}, \rho_{22}] = [0, 0, 0, 0]$ (IID) (black lines)

$$Ro = [\rho_{11}, \rho_{12}, \rho_{21}, \rho_{22}] = [0.5, 0.5, 0.5, 0.5] \text{ (blue lines)}$$

$$Ro = [\rho_{11}, \rho_{12}, \rho_{21}, \rho_{22}] = [0.8, 0.8, 0.8, 0.8] \text{ (red lines)}$$

In Figures 1-2, we show Monte-Carlo simulation results for parametric detectors (dotted lines) and permutation detectors (continuous lines) under nonfluctuating target model (NF). Parameters of logarithmic and clipping detectors are $\alpha=32$ and $A=2$ (for parametric and permutation clipping detectors), respectively. Detector thresholds are the correspond-

ing ones to IID conditions: $[0,0;0,0]$ with $P_{fa}=10^{-3}$. The shape parameter considered in this case is: $\nu=0.5$ (spiky clutter). It is apparent that the correlation coefficients have a significant importance in detector performances (see Figure 1).

As the azimuth correlation coefficients ρ_{21} and ρ_{22} increase, the P_{fa} of all detectors increases, too (remember that if $SCR \rightarrow 0$ ($-\infty$ dB), then $P_d \rightarrow P_{fa}$); although the P_d for $P_d > 0.2$ is little sensitive to ρ_{21} and ρ_{22} variations. For the best permutation detector (clipping), detectability losses with respect to the best parametric detector and for $0.2 \leq Pd \leq 0.8$ increase from 0.5 dB (for $R_o = [0,0;0,0]$) to 1.5 dB (for $R_o = [0,0;0.9,0.9]$). On the other hand, the correlation coefficients "in range" ρ_{11} and ρ_{12} have a beneficial effect over performances: P_{fa} stays constant and P_d (in the interval of interest) increases as ρ_{11} and ρ_{12} increase, as you can see in Figure 2. For the best permutation detector, detectability losses with respect to the best parametric detector and for $0.2 \leq Pd \leq 0.8$ decrease from 0.5 dB (for $R_o = [0,0;0,0]$) to 0 dB (for $R_o = [0.9,0.9;0,0]$). Also, we have observed that in the case of azimuthal correlation, performances of any detector have similar sensitivity with respect to ρ_{22} that with respect to ρ_{21} ; also, for correlation in range, ρ_{12} has a similar effect that ρ_{11} .

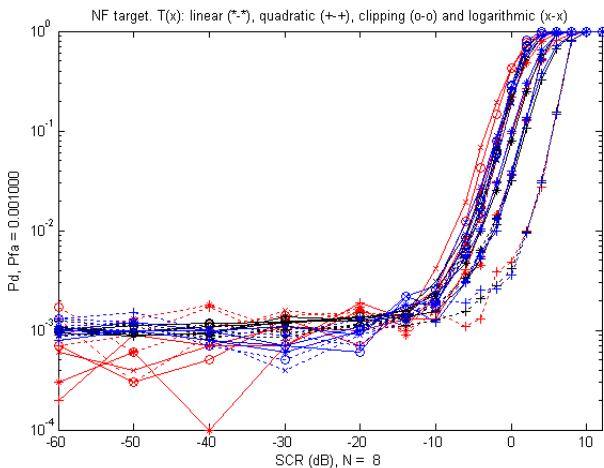


Figure 2 - Detection probability (P_d) versus SCR for parametric (dotted lines) and permutation (continuous lines) detectors ($N=8$ and $M=7$), under correlated spiky clutter ($\nu=0.5$) and nonfluctuating target model (NF). Clutter correlation coefficients:

$$R_o = [\rho_{11}, \rho_{12}; \rho_{21}, \rho_{22}] = [0, 0; 0, 0] \text{ (IID) (black lines)}$$

$$R_o = [\rho_{11}, \rho_{12}; \rho_{21}, \rho_{22}] = [0.5, 0.5; 0, 0] \text{ (blue lines)}$$

$$R_o = [\rho_{11}, \rho_{12}; \rho_{21}, \rho_{22}] = [0.8, 0.8; 0, 0] \text{ (red lines)}$$

In Figures 3-4, we show Monte-Carlo simulation results for the parametric detectors (dotted lines) and the permutation detectors (continuous lines) under Swerling II target model (SW-II). Parameters of logarithmic and clipping detectors are $\alpha=32$ and $A=2.6$ (for the parametric clipping detector) and $A=3.2$ (for the permutation clipping detector). Detector thresholds are the corresponding ones to IID conditions: $[0,0;0,0]$ with $P_{fa}=10^{-3}$. The shape parameter considered is:

$\nu=0.5$ (spiky clutter). Also, it is apparent that the correlation coefficients have a significant importance in detector performances (see Figure 3).

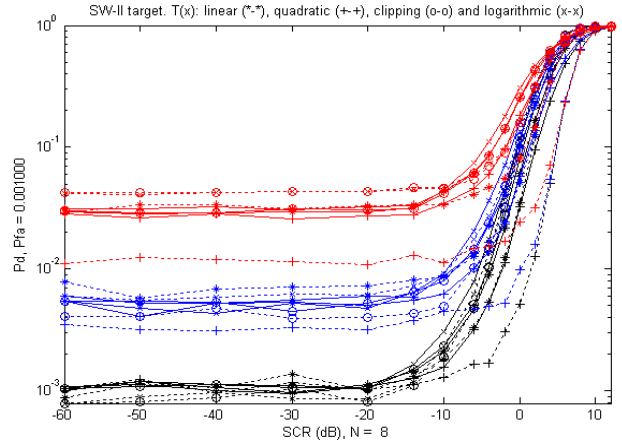


Figure 3 - Detection probability (P_d) versus SCR for parametric (dotted lines) and permutation (continuous lines) detectors ($N=8$ and $M=7$), under correlated spiky clutter ($\nu=0.5$) and Swerling II target model (SW-II). Clutter correlation coefficients:

$$R_o = [\rho_{11}, \rho_{12}; \rho_{21}, \rho_{22}] = [0, 0; 0, 0] \text{ (IID) (black lines)}$$

$$R_o = [\rho_{11}, \rho_{12}; \rho_{21}, \rho_{22}] = [0.5, 0.5; 0.5, 0.5] \text{ (blue lines)}$$

$$R_o = [\rho_{11}, \rho_{12}; \rho_{21}, \rho_{22}] = [0.8, 0.8; 0.8, 0.8] \text{ (red lines)}$$

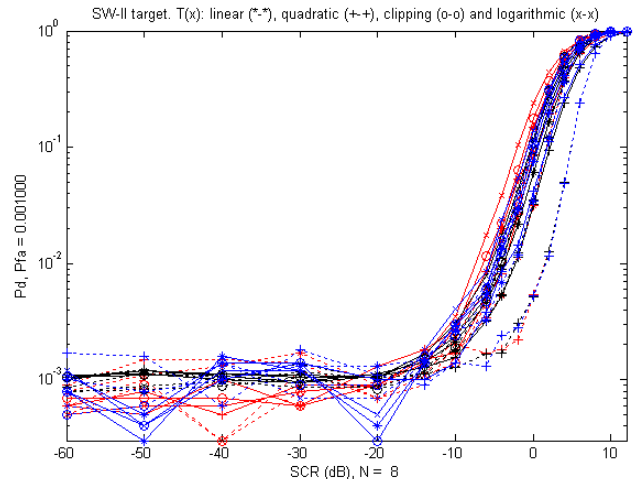


Figure 4 - Detection probability (P_d) versus SCR for parametric (dotted lines) and permutation (continuous lines) detectors ($N=8$ and $M=7$), under correlated spiky clutter ($\nu=0.5$) and Swerling II target model (SW-II). Clutter correlation coefficients:

$$R_o = [\rho_{11}, \rho_{12}; \rho_{21}, \rho_{22}] = [0, 0; 0, 0] \text{ (IID) (black lines)}$$

$$R_o = [\rho_{11}, \rho_{12}; \rho_{21}, \rho_{22}] = [0.5, 0.5; 0, 0] \text{ (blue lines)}$$

$$R_o = [\rho_{11}, \rho_{12}; \rho_{21}, \rho_{22}] = [0.8, 0.8; 0, 0] \text{ (red lines)}$$

Note also that as the azimuth correlation coefficients ρ_{21} and ρ_{22} increase, the false alarm probability (P_{fa}) of all detectors increases, too; although the detection probability (P_d) for $P_d > 0.2$ is little sensitive to ρ_{21} and ρ_{22} variations. For the best permutation detector (logarithmic and clipping), detectability losses with respect to the best parametric detector and for $0.2 \leq Pd \leq 0.8$ increase from 0.8 dB (for

$R_o = [0, 0; 0, 0]$ to 1.5 dB (for $R_o = [0, 0; 0.9, 0.9]$). On the other hand, the correlation coefficients “in range” ρ_{11} and ρ_{12} have a beneficial effect over performances: P_{fa} stays constant and P_d (in the interval of interest) increases as ρ_{11} and ρ_{12} increase, as you can see in Figure 4. For the best permutation detector, detectability losses with respect to the best parametric detector and for $0.2 \leq P_d \leq 0.8$ decrease from 0.8 dB (for $R_o = [0, 0; 0, 0]$) to 0 dB (for $R_o = [0.9, 0.9; 0, 0]$). Also, we have observed that in the case of azimuthal correlation, the performance of any detector has similar sensitivity to ρ_{22} than to ρ_{21} ; also, for correlation in range, ρ_{12} has similar effect than ρ_{11} .

In Figures 5-6, we show Monte-Carlo simulation results for the parametric detectors (dotted lines) and the permutation detectors (continuous lines) under nonfluctuating target model (NF). Parameters of logarithmic and clipping detectors are $\alpha=32$ and $A=2$ (for parametric and permutation clipping detectors), respectively. Detector thresholds are the corresponding ones to IID conditions: $[0, 0; 0, 0]$ with $P_{fa}=10^{-3}$. The shape parameter considered in this case is: $\nu = \infty$ (Rayleigh clutter). Also, it is apparent that the correlation coefficients have a significant importance in detector performances (see Figure 5).

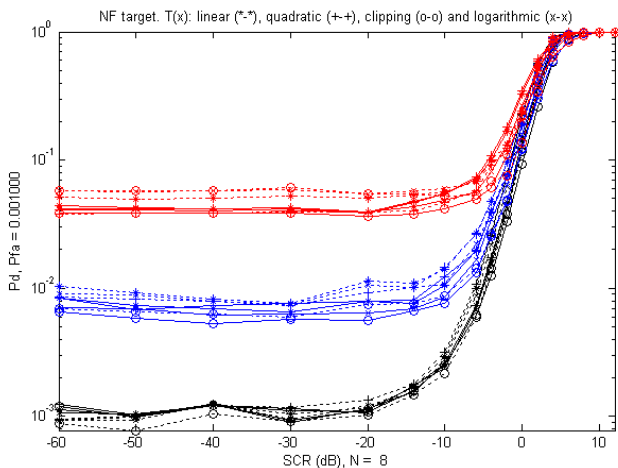


Figure 5 - Detection probability (P_d) versus SCR for parametric (dotted lines) and permutation (continuous lines) detectors ($N=8$ and $M=7$), under correlated Rayleigh clutter ($\nu=\infty$) and nonfluctuating target model (NF). Clutter correlation coefficients:

$$\begin{aligned}
 R_o &= [\rho_{11}, \rho_{12}; \rho_{21}, \rho_{22}] = [0, -; 0, -] \text{ (IID) (black lines)} \\
 R_o &= [\rho_{11}, \rho_{12}; \rho_{21}, \rho_{22}] = [0.5, -; 0.5, -] \text{ (blue lines)} \\
 R_o &= [\rho_{11}, \rho_{12}; \rho_{21}, \rho_{22}] = [0.8, -; 0.8, -] \text{ (red lines)}
 \end{aligned}$$

For Rayleigh clutter, as the azimuth correlation coefficient ρ_{21} increases (ρ_{22} is not necessary), the false alarm probability (P_{fa}) of all detectors increases, too; although the detection probability (P_d) for $P_d > 0.2$ is little sensitive to ρ_{21} variations. For the best permutation detector (linear), detectability losses with respect to the best parametric detector and for $0.2 \leq P_d \leq 0.8$ are about 0.8 dB from $R_o = [0, -; 0, -]$ to

$R_o = [0, -; 0.9, -]$. On the other hand, the correlation coefficient “in range” ρ_{11} (ρ_{12} is not necessary either) has a beneficial effect over performances: P_{fa} stays constant and P_d (in the interval of interest) increases as ρ_{11} increases, as you can see in Figure 6. For the best permutation detector, detectability losses with respect to the best parametric detector and for $0.2 \leq P_d \leq 0.8$ decrease from 0.8 dB (for $R_o = [0, -; 0, -]$) to 0 dB (for $R_o = [0.9, -; 0, -]$).

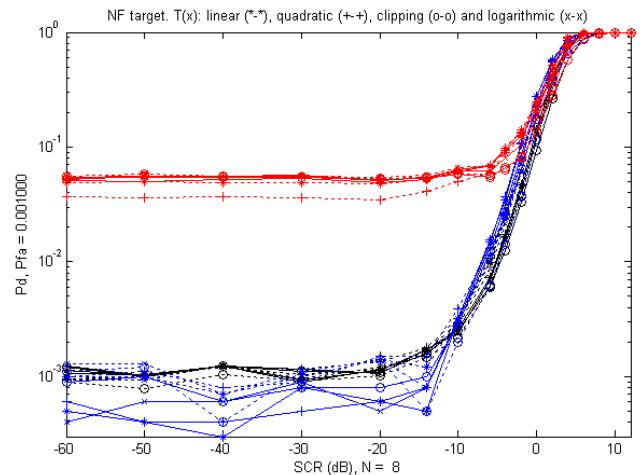


Figure 6 - Detection probability (P_d) versus SCR for parametric (dotted lines) and permutation (continuous lines) detectors ($N=8$ and $M=7$), under correlated Rayleigh clutter ($\nu=\infty$) and nonfluctuating target model (NF). Clutter correlation coefficients:

$$\begin{aligned}
 R_o &= [\rho_{11}, \rho_{12}; \rho_{21}, \rho_{22}] = [0, -; 0, -] \text{ (IID) (black lines)} \\
 R_o &= [\rho_{11}, \rho_{12}; \rho_{21}, \rho_{22}] = [0.8, -; 0, -] \text{ (blue lines)} \\
 R_o &= [\rho_{11}, \rho_{12}; \rho_{21}, \rho_{22}] = [0, -; 0.8, -] \text{ (red lines)}
 \end{aligned}$$

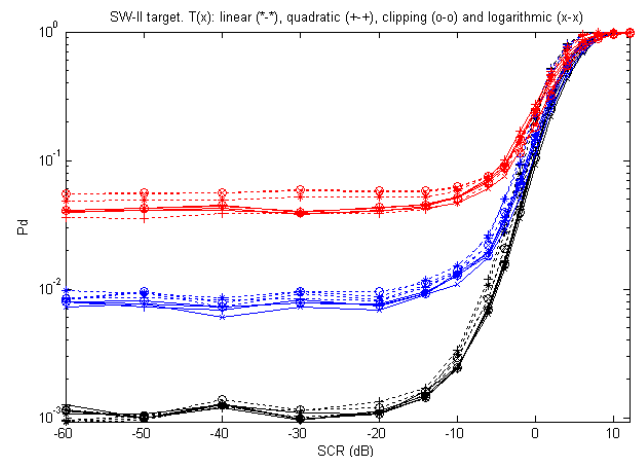


Figure 7 - Detection probability (P_d) versus SCR for parametric (dotted lines) and permutation (continuous lines) detectors ($N=8$ and $M=7$), under correlated Rayleigh clutter ($\nu=\infty$) and Swerling II target model (SW-II). Clutter correlation coefficients:

$$\begin{aligned}
 R_o &= [\rho_{11}, \rho_{12}; \rho_{21}, \rho_{22}] = [0, 0; 0, 0] \text{ (IID) (black lines)} \\
 R_o &= [\rho_{11}, \rho_{12}; \rho_{21}, \rho_{22}] = [0.5, -; 0.5, -] \text{ (blue lines)} \\
 R_o &= [\rho_{11}, \rho_{12}; \rho_{21}, \rho_{22}] = [0.8, -; 0.8, -] \text{ (red lines)}
 \end{aligned}$$

In Figs. 7-8, we show Monte-Carlo simulation results for the parametric detectors (dotted lines) and the permutation detectors (continuous lines) under Swerling II target model (SW-II). Parameters of logarithmic and clipping detectors are $\alpha=32$ and $A=2.6$ (for the parametric clipping detector) and $A=3.2$ (for the permutation clipping detector). Detector thresholds are the corresponding ones to IID conditions: $[0,0;0,0]$ with $P_{fa}=10^{-3}$. The shape parameter considered is $\nu=\infty$ (Rayleigh clutter). Also, it is apparent that the correlation coefficients have a significant importance in detector performances (see Figure 7).

Also, in this case, as the azimuth correlation coefficient ρ_{21} increases, the false alarm probability (P_{fa}) of all detectors increases, too; although the detection probability (P_d) for $P_d > 0.2$ is little sensitive to ρ_{21} variations. For the best permutation detector (quadratic), detectability losses with respect to the best parametric detector and for $0.2 \leq P_d \leq 0.8$ are about 1.8 dB from $R_o = [0, -, 0, -]$ to $R_o = [0, -, 0.9, -]$. On the other hand, the correlation coefficient “in range” ρ_{11} has a beneficial effect over performances: P_{fa} stays constant and P_d (in the interval of interest) increases as ρ_{11} increases, as you can see in Figure 8. For the best permutation detector, detectability losses with respect to the best parametric detector and for $0.2 \leq P_d \leq 0.8$ decrease from 1.8 dB (for $R_o = [0, -, 0, -]$) to 1 dB (for $R_o = [0.9, -, 0, -]$).

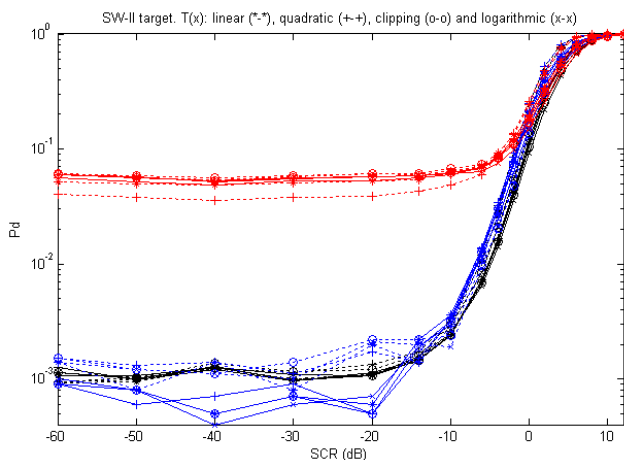


Figure 8 - Detection probability (P_d) versus SCR for parametric (dotted lines) and permutation (continuous lines) detectors ($N=8$ and $M=7$), under correlated Rayleigh clutter ($\nu=\infty$) and Swerling II target model (SW-II). Clutter correlation coefficients:

$$R_o = [\rho_{11}, \rho_{12}; \rho_{21}, \rho_{22}] = [0, 0; 0, 0] \text{ (IID) (black lines)}$$

$$R_o = [\rho_{11}, \rho_{12}; \rho_{21}, \rho_{22}] = [0.8, -, 0, -] \text{ (blue lines)}$$

$$R_o = [\rho_{11}, \rho_{12}; \rho_{21}, \rho_{22}] = [0, -, 0.8, -] \text{ (red lines)}$$

Finally, similar results have been obtained for other values of P_{fa} , N and M .

4. CONCLUSION

In this paper, we have showed some performance results of four permutation detectors (linear, quadratic, logarithmic and clipping), under correlated clutter; also, we have considered their parametric counterparts for comparisons. The most important conclusion is that azimuthal correlation of samples must be avoided in order to preserve good performances of the detectors. Preprocessing of clutter samples has to be done in order to reduce azimuthal correlation (using frequency agility, pulse-to-pulse polarization changing, clutter cancellation, etc.). Note that if the azimuthal correlation is too high, a block of N pulses has the same information of one single pulse (supposing a nonfluctuating target model), i.e. the detector performance has no gain with N integrated pulses highly correlated against one single pulse.

REFERENCES

- [1] J.E. González-García, J.L. Sanz-González, and F. Álvarez-Vaquero. “Nonparametric permutation tests versus parametric tests in radar detection under K-distributed clutter”, *Proc. IEEE Int. Radar Conf. 2005 (RADAR 2005)*, Arlington (USA), May 2005. (S12-2), pp. 250-255.
- [2] J.L. Sanz-González and F. Álvarez-Vaquero, “Nonparametric rank detectors under K-distributed clutter in radar applications”, *IEEE Trans. on Aerospace and Electronic Systems*, Vol. 41 (2), April 2005, pp. 702-710.
- [3] S. Watts. “Radar detection prediction in sea clutter using the compound K-distribution model”, *IEE Proceedings, Part F (Radar and Signal Processing)*, 132 (7), Dec. 1985, pp. 613-620.
- [4] Conte, E., and Longo, M. “Characterization of radar clutter as a spherically invariant random process”, *IEE Proceedings, Part F (Radar and Signal Processing)*, Vol. 134, No. 2, April 1987, pp.191-197.
- [5] M. Rangaswamy, D. Weiner and A. Öztürk. “Non-Gaussian random vector identification using spherically invariant random processes”, *IEEE Trans. on Aerospace and Electronic Systems*, 29 (1), 1993, pp. 111-124.
- [6] M. Rangaswamy. “Spherically invariant random processes for modeling non-Gaussian radar clutter”, *Record of the 27th Asilomar Conf. on Signal, Systems and Computers*, Pacific Grove (USA), Vol. 2, Nov. 1993, pp. 1106-1110.
- [7] J.E. González-García, J.L. Sanz-González, and F. Álvarez-Vaquero. “Optimal detectors for nonfluctuating targets under spiky K-distributed clutter in radar applications”, *Proc. Third IEEE Sensor Array and Multichannel Signal Processing Workshop (SAM-2004)*, Sitges (Spain), July 2004. (S4-1) pp. 191-195.